THE JOURNAL OF BIOLOGICAL CHEMISTRY VOL. 285, NO. 49, pp. 38389–38398, December 3, 2010

Noncanonical Tandem SH2 Enables Interaction of Elongation Factor Spt6 with RNA Polymerase II*[S]

Received for publication, May 20, 2010, and in revised form, August 25, 2010 Published, JBC Papers in Press, October 6, 2010, DOI 10.1074/jbc.M110.146696

Marie-Laure Diebold[‡], Erin Loeliger[§], Michael Koch[‡1], Fred Winston[§], Jean Cavarelli[‡], and Christophe Romier[‡2]

From the [‡]Département de Biologie et Génomique Structurales, Institut de Génétique et Biologie Moléculaire et Cellulaire, Université de Strasbourg, CNRS, INSERM, 1 rue Laurent Fries, B.P. 10142, 67404 Illkirch Cedex, France and the [§]Department of Genetics, Harvard Medical School, Boston, Massachusetts 02115

Src homology 2 (SH2) domains are mostly found in multicellular organisms where they recognize phosphotyrosine-containing signaling proteins. Spt6, a conserved transcription factor and putative histone chaperone, contains a C-terminal SH2 domain conserved from yeast to human. In mammals, this SH2 domain recognizes phosphoserines rather than phosphotyrosines and is essential for the recruitment of Spt6 by elongating RNA polymerase II (RNAPII), enabling Spt6 to participate in the coupling of transcription elongation, chromatin modulation, and mRNA export. We have determined the structure of the entire Spt6 C-terminal region from *Antonospora locustae*, revealing the presence of two highly conserved tandem SH2 domains rather than a single SH2 domain. Although the first SH2 domain has a canonical organization, the second SH2 domain is highly noncanonical and appears to be unique in the SH2 family. However, both SH2 domains have phosphate-binding determinants. Our biochemical and genetic data demonstrate that the complete tandem, but not the individual SH2 domains, are necessary and sufficient for the interaction of Spt6 with RNAPII and are important for Spt6 function *in vivo*. Furthermore, our data suggest that binding of RNAPII to the Spt6 tandem SH2 is more extensive than the mere recognition of a doubly phosphorylated C-terminal domain peptide by the tandem SH2. Taken together, our results show that Spt6 interaction with RNAPII via a novel arrangement of canonical and noncanonical SH2 domains is crucial for Spt6 function *in vivo*.

Transcription elongation by the eukaryotic RNA polymerase II (RNAPII)[3] is tightly linked to chromatin modulation and mRNA processing and export (1–3). The various factors involved in these mechanisms are often recruited directly by RNAPII through the docking platform provided by the C-terminal domain (CTD) of its largest subunit, Rpb1. The CTD is composed of a large number of heptad repeats which are generally composed of the canonical motif $Tyr^1Ser^2Pro^3Thr^4Ser^5Pro^6Ser^7$, although some repeats may diverge from this consensus sequence (4).

During the transcription cycle, the CTD repeats undergo a large number of phosphorylation and dephosphorylation events, notably at their serine residues (Ser^2, Ser^5, and Ser^7). These changes in the CTD phosphorylation pattern alter its binding surface as transcription proceeds and enable the recruitment by RNAPII of different sets of factors at each transcriptional stage (5–8). The ability of the CTD to recruit multiple activities is essential for the coupling of transcription with chromatin modulation and mRNA processing and export. One such activity recruited by the CTD that plays essential roles is the Spt6/Iws1 complex.

The essential protein Spt6 is a putative histone chaperone that interacts with histone H3 and promotes the reassembly of nucleosomes on promoters and on the body of genes in the wake of the RNAPII (9–13). Depletion of Spt6 causes sustained transcription in repressing conditions and production of aberrant transcripts due to initiation from cryptic sites within the body of genes (13, 14). Spt6 also belongs to the family of elongation factors, enhancing the elongation rates of RNAPII both *in vitro* and *in vivo* (15–17). Yet, this latter role appears independent of Spt6 chaperone activity because elongation enhancement occurs also on naked DNA templates (16, 17).

The association of Spt6 with the essential protein Iws1/Spn1 (17–22) provides an additional link between Spt6, chromatin modulation, and mRNA export. Indeed, mammalian Iws1 is required for the recruitment of the lysine methyltransferase HYPB/Setd2 that trimethylates H3K36 across transcribed regions. In addition, Iws1 also interacts directly with the export factor REF1/Aly, with the depletion of Iws1 leading to splicing defects and nuclear retention of bulk poly(A)$^+$ mRNAs (17, 23).

Several lines of evidence indicate that the Spt6/Iws1 complex travels with RNAPII. In yeast, both Spt6 and Iws1 have been shown by ChIP analyses to be present on the promoter, the body, and even past the polyadenylation signal of several genes (24). In agreement with these results, *Drosophila* Spt6 colocalizes with hyperphosphorylated RNAPII at transcribed genes (25–28). More recently, a direct interaction of mammalian Spt6 with the RNAPII CTD has been characterized which requires the SH2 motif found in the Spt6 C-terminal region (17, 23). A mutation in this motif leads to the loss of the inter-

* This work was supported, in whole or in part, by National Institutes of Health Grant GM32967. This work was also supported by the CNRS, INSERM, the Université de Strasbourg, and the European Commission SPINE2-Complexes Contract LSHG-CT-2006-031220.

[S] The on-line version of this article (available at http://www.jbc.org) contains supplemental Tables 1 and 2 and Figs. 1–5.

[1] Present address: Institut für Biochemie, Universität zu Köln, Otto-Fischer-Str. 12–14, 50674 Köln, Germany.

[2] To whom correspondence should be addressed. Tel.: 33-3-88-65-57-98; Fax: 33-3-88-65-32-79; E-mail: romier@igbmc.fr.

[3] The abbreviations used are: RNAPII, RNA polymerase II; al, *A. locustae*; cg, *C. glabrata*; CTD, C-terminal domain; ec, *E. cuniculi*; hs, Homo sapiens; *sc*, *Saccharomyces cerevisiae*; TAP, tandem affinity purification.

action of Spt6 with the polymerase and causes splicing defects (17).

SH2 motifs are generally found in signaling proteins from higher eukaryotes where they are involved in the specific recognition of phosphotyrosine-containing proteins (29). Phosphate recognition is carried out by several residues, including an invariant arginine on strand βB of the SH2 motif as well as various residues of the BC loop connecting the strands βB and βC of the SH2 motif (30). Yet, phosphotyrosine binding is not sufficient for specific target recognition which also requires interaction with flanking residues (31, 32). Specificity can be reinforced by contacts of the SH2 domain with other regions of the target protein (33) or the use of tandem SH2 domains (34, 35).

Surprisingly, the Spt6-RNAPII interaction requires the hyperphosphorylation of the CTD repeats on a serine (Ser^2) rather than a tyrosine residue, suggesting that the Spt6 SH2 motif represents an ancient SH2 domain recognizing phosphoserines rather than phosphotyrosines (17, 23). The conservation of this SH2 domain throughout evolution highlights its functional importance (36). Spt6 appears to be the only protein in yeast harboring an SH2 domain.

The recent structure of the SH2 domain of Spt6 from *Candida glabrata* has revealed a rather canonical organization for this domain (37). Notably, the conservation of the invariant arginine on the βB strand and the presence of residues in the BC loop that might participate in phosphate recognition are in agreement with phosphoresidue binding by this SH2 domain. Yet, the absence of residues being able to form amino-aromatic interactions with an incoming phosphotyrosine as well as a shallower phosphoresidue-binding pocket suggested a favored recognition of phosphoserines over phosphotyrosines. However, binding assays *in vitro* showed that the yeast and human Spt6 SH2 domains are unable to interact with a single or tandem CTD repeats phosphorylated on Ser^2 (37).

These results suggest that the entire conserved C-terminal region of Spt6 rather than the single SH2 motif is required for binding to the RNAPII CTD. We have solved the structure of the entire C-terminal region of Spt6 from the yeast-related organism *Antonospora locustae* at 2.2 Å resolution. Unexpectedly, the structure reveals that this region is formed by two SH2 domains arranged in tandem. Whereas the first SH2 domain shows a canonical organization, the second SH2 domain displays many atypical features at the sequence and structural levels. Yet both SH2 domains have retained determinants for phosphate binding. By performing GST pulldown assays on yeast extract, we show that the tandem, but not the individual SH2 domains, is able to interact with RNAPII. Furthermore, deletion of either the two SH2 domains or only the second SH2 domain causes severe mutant phenotypes *in vivo*, confirming the importance of the tandem SH2 domain. In addition, mutation of putative phospho-binding residues in both SH2 domains decreases but does not fully abolish interaction with RNAPII, suggesting an extensive interaction between the Spt6 tandem SH2 and RNAPII. In agreement, short phosphorylated CTD fragments are unable to bind to the tandem SH2. Altogether, our data reveal the presence of an unexpected, atypical tandem SH2 within Spt6, emphasizing the importance of both the canonical and the noncanonical SH2 domains for Spt6 function *in vivo*.

EXPERIMENTAL PROCEDURES

Cloning and Purification—All constructs used in this study were amplified by PCR techniques and cloned using NdeI and BamHI restriction sites into either the pnEA-tH expression vector from the pET-MCN series (38), which encodes an N-terminal His_6 tag and a thrombin cleavage site, or a modified pGEX-4T2 vector containing compatible restriction sites. All proteins were overexpressed in *Escherichia coli* BL21[DE3] in 2LB medium in the presence of the pRARE2 vector (Novagen). When the cultures reached an $A_{600\ nm}$ of 0.4 they were cooled to 25 °C, and gene expression was induced for 16 h at 25 °C with 0.7 mM isopropyl-β-D-thiogalactopyranoside (Euromedex). Cells were then harvested and resuspended in a lysis buffer containing 10 mM Tris (pH 8.0) and either 50 or 400 mM NaCl.

For structural studies, the Spt6 C-terminal regions from *Encephalitozoon cuniculi* (ec; residues 724–894) and *A. locustae* (al; residues 783–957) were used. The cells were lysed by sonication in a lysis buffer containing 400 mM NaCl. The soluble fraction was incubated for 1 h with 500 μl of Talon affinity resin (Clontech). The beads were then washed and resuspended in lysis buffer, and bovine thrombin was added overnight for cleaving off the histidine tag. The proteins were then injected onto a gel filtration column Hiload 16/60 Superdex 75 (GE Healthcare) equilibrated with lysis buffer supplemented with 2 mM dithiothreitol (Euromedex). The purified proteins were concentrated on the Amicon 10 K system (Millipore) to a concentration of 20 mg/ml.

Crystallization and Data Collection—Crystallization trials were performed using the hanging-drop vapor-diffusion method at 24 °C by mixing equal amounts of protein and crystallization buffer. Crystals for the C-terminal region of *A. locustae* Spt6 were obtained in presence of 0.1 M MES (pH 6.0), 1.5 M ammonium sulfate, and 20 mM $CoCl_2$. For data collection, crystals were frozen in liquid nitrogen in a cryoprotectant solution containing 0.1 M MES (pH 6.0), 1.5 M ammonium sulfate, 15 mM $CoCl_2$, and 25% xylitol. All data collections were performed at 100 K. A native data set was collected on ESRF beamline ID29 at a wavelength of 0.9762 Å. The derivative data sets were collected on ESRF beamline ID14-2 at a wavelength of 0.933 Å.

Structure Determination and Refinement—Structure determination was carried out using heavy atom derivatives. Native crystals were soaked overnight in the presence of either 1 mM $KAu(CN)_2$ or 1 mM $(CH_3)_3PbAc$ and then frozen in the same cryoprotectant solution used for native crystals. All data were processed with HKL2000 (39). Phase determination by MIRAS was carried out using Auto-SHARP (40) including solvent modification with SOLOMON (41). Model building was performed using TURBO-FRODO and COOT (42). Refinement was done using REFMAC (43). There is one molecule per asymmetric unit. The final refined model has an R_{factor} and an R_{free} of 22.5% and 26.6%, with good deviations from ideal geometry (supplemental Table 1). Ramachandran

analysis shows 97.7% of residues in favored regions and 2.3% of residues in allowed regions. The refined model and the structure factor amplitudes have been deposited in the Protein Data Bank under the PDB code 2XP1.

GST Pulldown Experiments—Yeast extracts were prepared as described previously (44). The GST-fused proteins were lysed in a lysis buffer containing 10 mM Tris (pH 8.0) and 50 mM NaCl. The soluble cellular extract was incubated for 1 h with 50 μl of glutathione-Sepharose 4B resin (Amersham Biosciences). The beads were then washed several times in lysis buffer. The amounts of each construct were assessed by SDS-PAGE and Coomassie staining. To perform the pulldown, equivalent amounts of protein bound to the resin were incubated for 2 h in 30 μl of yeast extract. After incubation, beads were washed twice with a buffer containing 50 mM potassium chloride, 20 mM K-HEPES (pH 7.9), 0.2 mM EDTA, and 0.5 mM dithiothreitol and resuspended in 50 μl of Laemmli buffer. Retention of the largest subunit of the RNAPII was checked by Western blotting using the 7C2 antibody (45) directed against its CTD. Phospho-specificity was assessed using the H5 (Ser^2-phospho) and H14 (Ser^5-phospho) antibodies (Covance).

Yeast Strain Construction—All TAP-tagged alleles were created by transforming a *TAP-NatMx* cassette (amplified from pFA6a-C-TAP4-natMX6 (46)) into diploid strain FY2808 (supplemental Table 2). Nat^R transformants were isolated, and the TAP-tagged constructs were confirmed by PCR and sequencing. The *spt6-ΔTandem::TAP* is deleted for the last 201 codons of *SPT6*, encoding the two SH2 domains. The *spt6-Δ$SH2_2$::TAP* is deleted for the last 101 codons of *SPT6*, encoding the *$SH2_2$* domain. Sporulation and tetrad dissection were performed by standard procedures to analyze haploid strains that contained the deletions (47). For *SPT6::TAP* (full-length *SPT6* fused to TAP), cells behaved identically to wild-type cells (a wild-type growth rate and no *spt6* mutant phenotypes detected). Spot tests were performed on the following media: YPD, YPD at 37 °C, YPD at 16 °C, SC-His, SC-Lys, YPD + 150 mM hydroxyurea, YPD + 13 μg/ml phleomycin, and YPD + 15 mM caffeine. YPD, SC-His, and SC-Lys were made as described previously (47).

Western Blot Analysis—Protein extracts were prepared from strains FY653, FY2796, FY2797, and FY2798 as described previously (48). The TAP tag was detected using the peroxidase anti-peroxidase antibody (1:5000 dilution; Sigma). Spt6 antiserum was a generous gift from Laura McCollough and Tim Formosa (1:2000 dilution in TBST). Pgk1 was used as a loading control and visualized with anti-Pgk1 antiserum (Invitrogen 459250).

RESULTS

Spt6 C-terminal Region Contains Tandem SH2 Domains—The structural and biochemical characterization of the conserved Spt6 C-terminal region has been performed using Spt6 proteins from the fungi-related intracellular parasites *E. cuniculi* and *A. locustae*. The proteins of these organisms are smaller than their orthologs from other organisms, facilitating biochemical and structural analyses, although they retain the essential organization of their orthologs (49, 50). The *A. locustae* construct could be expressed in *E. coli*, purified to homogeneity and yielding well diffracting crystals. Structure determination was carried out by soaking native crystals with heavy atom derivatives, and the phase problem was solved by MIRAS. The initial model built in the experimental map was refined against a native dataset at 2.2 Å resolution to an R_{factor} of 22.5% and an R_{free} of 26.6%, with good deviations from ideal geometry (supplemental Table 1).

The structure reveals that the C-terminal region of Spt6 does not contain a single SH2 domain but is actually formed by two SH2 domains arranged in tandem, forming a single structural domain (Fig. 1). The presence of an SH2 motif in the second half of the Spt6 C-terminal region was unambiguously assessed by a structural homology search with DALI (51) and is clearly indicated by its secondary structure organization. The two SH2 domains ($SH2_1$ and $SH2_2$) are composed of a central three-stranded antiparallel β-sheet (strands βB–βD) sandwiched between N- and C-terminal α-helices (helices αA and αB). The central β-sheets are complemented by a smaller β-hairpin (strands βE–βF), reminiscent of the SRC family of SH2 motifs (30).

A specific feature of this tandem SH2 domain is the αB_1 helix of $SH2_1$ which is much longer than in standard SH2 domains. Although the N terminus of this helix forms canonical interactions with the $SH2_1$, its C-terminal extremity also makes extensive, mostly hydrophobic, interactions with $SH2_2$ (Fig. 1*A*). A kink in the second helical turn of this helix, due to an additional residue (Tyr^{865}), further brings the two SH2 domains in close vicinity, enabling the interaction between the strands βC_1 and βD_1 of the $SH2_1$ and the loop BC_2 of the $SH2_2$, thus expanding the hydrophobic core made between αB_1 and the $SH2_2$. Therefore, the long αB_1 helix is essential in providing the scaffold of the tandem SH2. Consequently, both SH2 domains are arranged almost head-to-tail with the two putative phosphoresidue-binding pockets exposed on the same face of the molecule (Fig. 1*A*).

$SH2_1$ Displays Mostly Canonical Features—Structural analysis of the $SH2_1$ domain shows that the canonical nature of this domain extends beyond its overall fold. First, an arginine is present on strand βB_1 (Arg^{817}) at the bottom of the phosphoresidue-binding pocket (Fig. 2*A*). An arginine at this position is normally involved in phosphate recognition and represents the only invariant signature of SH2 motifs (30). Second, Arg^{817} forms a hydrogen bond network with His^{838} on strand βD1 and Glu^{804} on helix αA_1, a network often observed in SH2 domains (Fig. 2*A*). Third, the BC_1 loop contains residues that are compatible with phosphate recognition (*e.g.* Ser^{820}). The same applies for Lys^{840}, on the βD_1 strand, which would be perfectly positioned for forming amino-aromatic interactions but which has not been conserved during evolution. On the other hand, as suggested upon the resolution of the *C. glabrata* (cg) $SH2_1$ structure, the absence of a residue on the helix αA_1 that may form amino-aromatic interactions with a phosphotyrosine, as well as a shallower phosphoresidue-binding pocket, could explain a favored binding of phosphoserine over phosphotyrosine (37).

Many SH2 domains recognize specifically incoming phosphoproteins by a two-pronged mechanism, where another

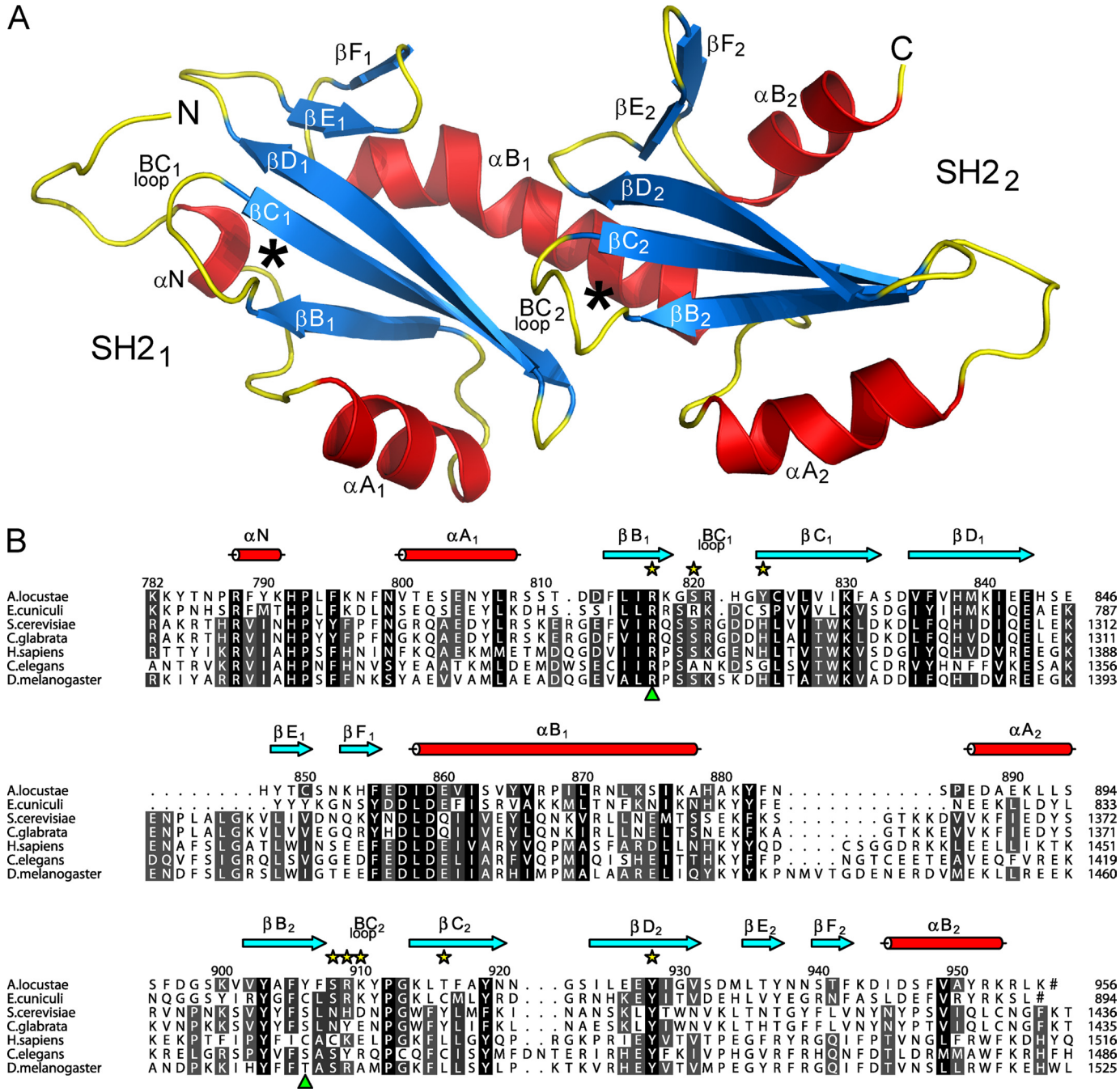

FIGURE 1. **Structure and sequence alignment of the conserved C-terminal region of Spt6.** *A*, *ribbon representation* of the *A. locustae* Spt6 tandem SH2 structure. α-Helices are colored in *red*, β-strands in *blue*, and loops in *yellow*. The putative phosphoresidue-binding pockets of the two SH2 domains are marked with an *asterisk* (*). Secondary structure elements throughout the figures are labeled according to the common SH2 nomenclature (30). All structural figures were created with PyMOL (Delano Scientific). *B*, sequence alignment of the conserved C-terminal region of Spt6. Conservation patterns have been indicated by *darker shading* (55). Secondary structure elements observed in the *A. locustae* structure are displayed above the sequences as *red cylinders* (α-helices) and *blue arrows* (β-strands). *Numbering* above the sequences corresponds to *A. locustae*, whereas the *numbering* at the end of each row relates to the different organisms. Residues shown to coordinate sulfate ions in the structure are labeled with *yellow stars*. Residues found at the position of the invariant arginine on strand βB of canonical SH2 domains are marked with a *green triangle* underneath the sequences. Ends of sequences are marked with a *number sign* (#).

residue, often located in position +3 to the phosphotyrosine, is bound in a second pocket at the surface of the SH2 domain (30). The structure of the cgSH2$_1$ suggests the presence of such a second pocket which is partially contributed to by residues from the αB$_1$ helix (37). However, in the context of the tandem SH2, the residues of the αB$_1$ helix that participate in the pocket are different. This is notably due to the kinked conformation of this helix which is not observed in the cgSH2$_1$ structure, most likely because of the absence of constraints imposed by the SH2$_2$ (supplemental Fig. 1). Importantly, our structure reveals that this second binding pocket is complemented by residues of the BC$_2$ and DE$_2$ loops from the second SH2 domain. Consequently, this pocket appears more like a groove at the interface between

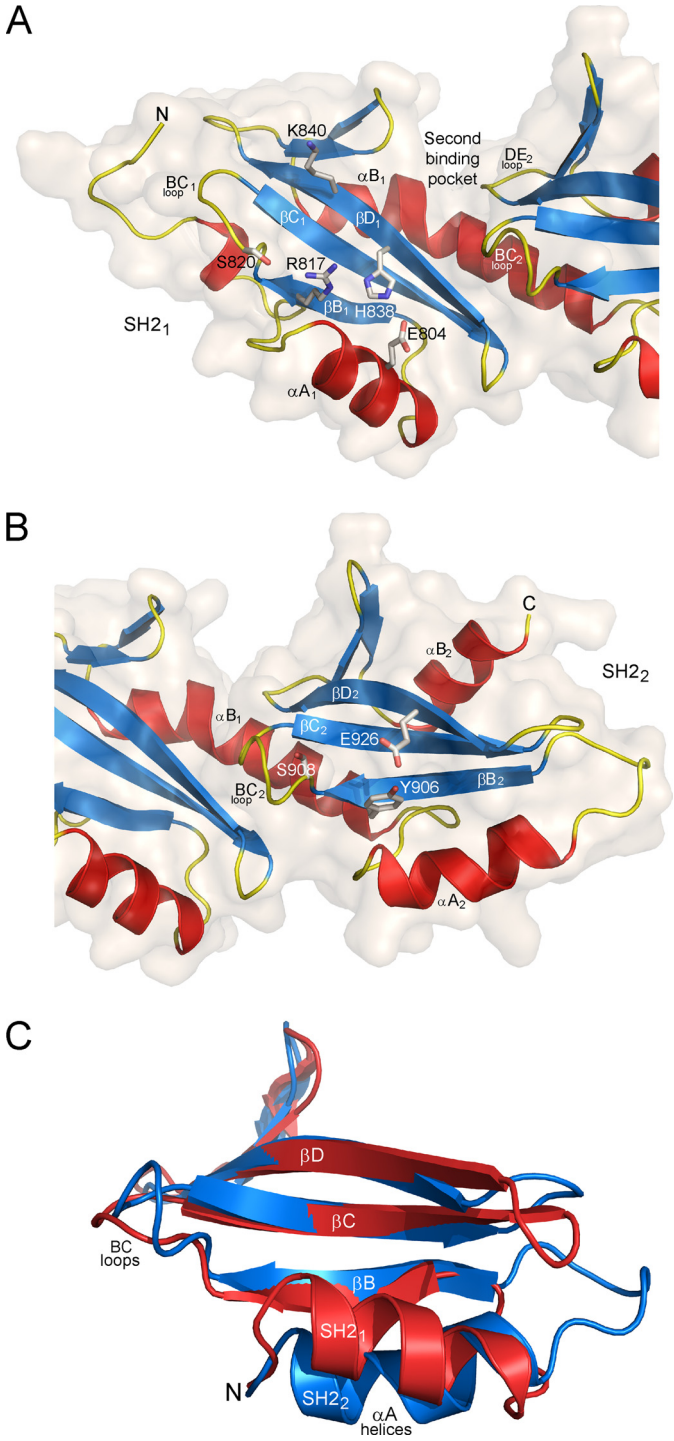

FIGURE 2. **Structural details of the $SH2_1$ and $SH2_2$ domains.** *A*, *ribbon representation* of the $SH2_1$ domain. The arginine (*R817*) that is invariant in canonical SH2 domains is shown as *sticks*. The two residues (*H838* and *E804*) forming a canonical hydrogen bond network with Arg^{817} are also shown as well as other residues (*S820* and *K840*) that might be involved in recognition of an incoming phosphoresidue. The surface of the $SH2_1$ domain is shown, highlighting the groove formed between the two SH2 domains that define the second binding pocket generally observed in canonical SH2 domains. *B*, *ribbon representation* of the $SH2_2$ domain. The tyrosine (*Y906*) that replaces the invariant arginine of canonical SH2 domains is shown as *sticks* as well as the glutamate (*E926*) forming a hydrogen bond with the hydroxyl of this tyrosine. The serine residue (*S908*) from the BC_2 loop that might be involved in recognition of an incoming phosphoresidue is also displayed. *C*, superposition of the $SH2_1$ (*red*) and $SH2_2$ (*blue*) domains, highlighting the difference of conformation between the two αA helices. For clarity, part of the N termini and the αB helices of the two domains has been removed.

the two SH2 domains where a peptide could make extensive interactions (Fig. 2*A*).

$SH2_2$ Is Highly Noncanonical—In strong contrast to $SH2_1$, the structural analysis of the second SH2 domain reveals atypical features despite conserved secondary structure elements. First, the phosphate-binding arginine found on strand βB in other SH2 domains is replaced here by a tyrosine (Tyr^{906}) (Fig. 2*B*). In our structure, the side chain of this tyrosine is not oriented toward the putative phosphate-binding pocket, but toward the carboxylate of Glu^{926} of strand βD_2, which forms a weak hydrogen bond with the hydroxyl of Tyr^{906}. These two residues have not been conserved during evolution. In particular, Tyr^{906} is generally replaced by smaller residues such as cysteine, threonine, or serine (Fig. 1*B*). This certainly explains why this second SH2 domain was not identified by sequence analyses. Second, residues on helix αA_2 and strand βD_2 that could form amino-aromatic interactions with a phosphotyrosine are also absent. Third, analysis of the $SH2_2$ surface does not give clear evidence for a second binding pocket, which could provide specificity in binding according to a two-pronged mechanism.

Another major difference observed in $SH2_2$ concerns the orientation of the helix αA_2 which runs parallel to the strand βB_2 rather than crossing over this strand as seen in canonical SH2 domains, including $SH2_1$ (Fig. 2*C*). In fact, a DALI search failed to find other SH2 domains with structural homology to $SH2_2$ with an αA helix adopting this conformation. A major effect of this conformational change is the opening of the putative phosphoresidue-binding pocket of the $SH2_2$ on the side where the αA_2 helix lies. This is reinforced by the absence of a residue on this helix that could form amino-aromatic interactions with a bound phosphotyrosine.

Phosphate Recognition by the Tandem SH2 Domains—The noncanonical nature of the $SH2_2$ domain clearly raised the question of the ability of this domain to recognize phosphopeptides. However, analysis of the electron density within the putative phosphate-binding pockets of both SH2 domains revealed the presence of additional density which was too large to accommodate single water molecules. Because the crystallization conditions contained sulfate ions that are known to bind readily into phosphate recognition pockets, we modeled two sulfate ions that fitted and refined perfectly into the density (Fig. 3, *A* and *B*, and supplemental Fig. 2). The specificity of this binding was confirmed by the fact that no other density for sulfate ion was observed in the rest of the structure and that the electrostatic potential at the surface of the tandem SH2 domains showed that both phosphate-binding pockets are positively charged (Fig. 3*C*).

Detailed analysis of the recognition of the sulfate ion by the $SH2_1$ shows that Arg^{817} makes a bidentate interaction with the sulfate (Fig. 3*A*). Further recognition of the sulfate involves interactions with the main chain amide and the hydroxyl of Ser^{820} on the BC_1 loop as well as the hydroxyl of Tyr^{824} from strand βC_1. All of these interactions are commonly used by canonical SH2 domains for phosphate recognition, with the exception of the one formed by Tyr^{824}, a residue that has not been conserved during evolution. However, superposition of the $alSH2_1$ and $cgSH2_1$ domains shows that

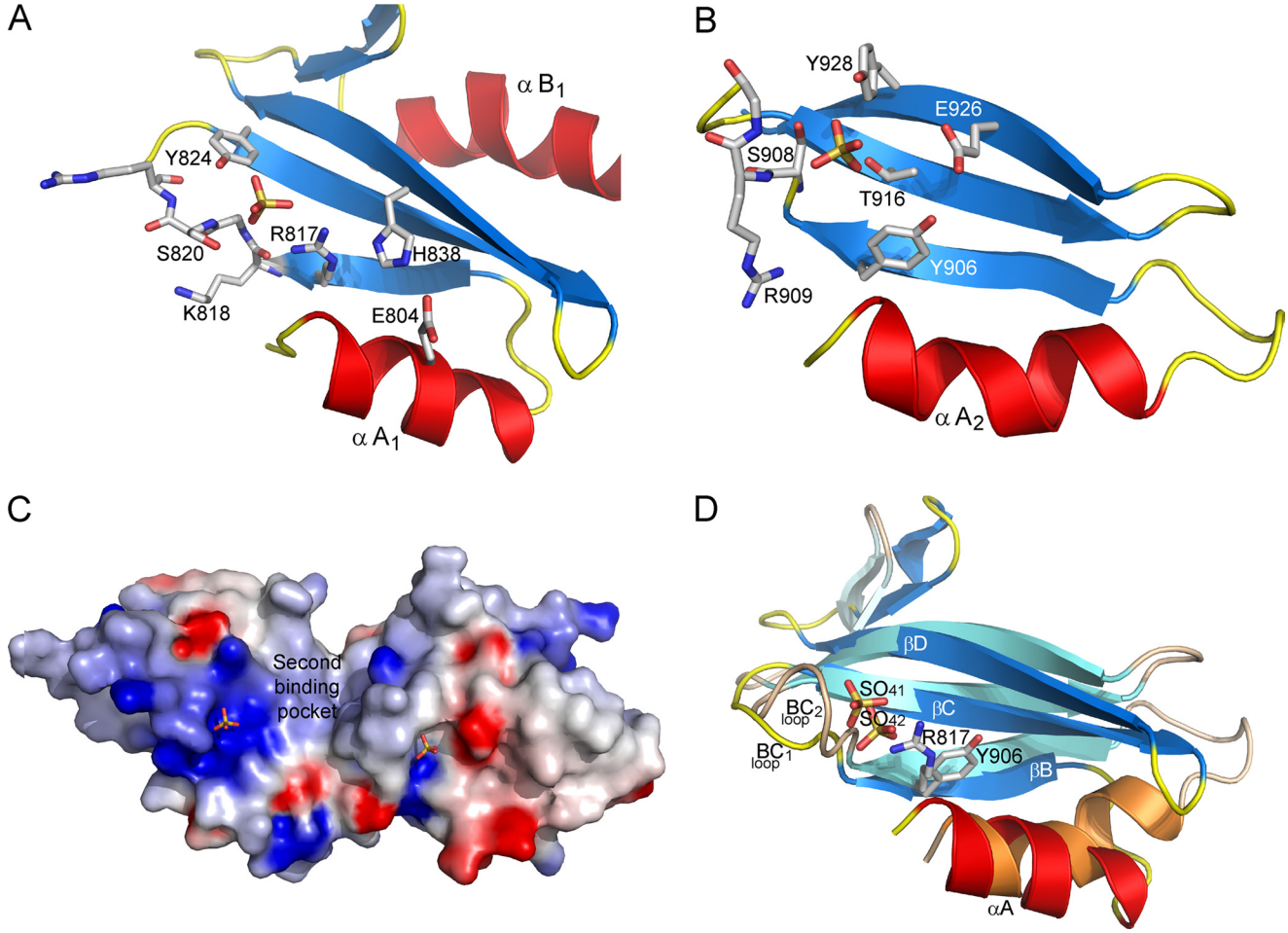

FIGURE 3. **Close-up views on sulfate recognition by the $SH2_1$ and $SH2_2$ domains.** Views of the phosphate-binding pockets of the $SH2_1$ (*A*) and the $SH2_2$ (*B*) domains. The domains are represented as *ribbons* with the exception of the central part of the BC loops, which are represented as *sticks*. The bound sulfate ions and the residues coordinating these ions are shown as *sticks* and *labeled*. *C*, electrostatic potential at the surface of the Spt6 tandem SH2 from *A. locustae*. The electrostatic potentials −8 and + 8 $k_B T$ (k_B, Boltzmann constant; *T*, temperature) are colored *red* and *blue*, respectively. The bound sulfate ions are shown as *sticks*. A direct path connecting the two phosphoresidue-binding pockets of the $SH2_1$ and $SH2_2$ domains can be observed. The position of the putative second binding pocket of the $SH2_1$ is *labeled*. *D*, superposition of the phosphate-binding pockets of the $SH2_1$ and $SH2_2$ domains. The bound sulfate ions (SO_{41} and SO_{42} for the $SH2_1$ and $SH2_2$ domains, respectively) as well as the side chains of Arg^{817} and Tyr^{906} are shown as *sticks*. Deeper positioning of the SO_{42} sulfate ion within the $SH2_2$ pocket is clearly seen. This is partly due to the absence of an arginine on strand βB_2 that would otherwise cause steric hindrance. For clarity, in *B* and *C*, the side chain of Lys^{910}, which extends over the phosphate-binding pocket of the $SH2_2$, has been removed.

the hydroxyl of Ser^{1283} in the BC_1 loop of the $cgSH2_1$ can perfectly play the role of the $alTyr^{824}$ hydroxyl (supplemental Fig. 3). These results confirm experimentally that the major determinants for canonical phosphate recognition are fully conserved in the Spt6 $SH2_1$ domain.

In contrast, sulfate recognition by the $SH2_2$ uses both canonical and noncanonical features. First, sulfate recognition involves interactions with the hydroxyl of Ser^{908} and the main chain amides of Arg^{909} and Lys^{910} from the BC_2 loop (Fig. 3*B*). However, in addition to these canonical features, the hydroxyl of Tyr^{906}, which replaces the otherwise invariant arginine on strand βB_2, does not interact with the sulfate ion. Compensating for this loss of interaction, two atypical interactions are formed with the hydroxyls of Thr^{916} on the βC_2 strand and Tyr^{928} on the βD_2 strand. Therefore, despite its noncanonical features, the $SH2_2$ appears to have kept determinants for phosphate recognition, these determinants reinforcing, however, the atypical character of this domain.

Interestingly, superposition of the $SH2_1$ and $SH2_2$ domains shows that the sulfate ion bound to the $SH2_2$ is located deeper within the phosphate-binding pocket, about 2 Å away from the position of the sulfate in the $SH2_1$ (Fig. 3*D*). This shift is due to a different conformation of the BC_2 loop and to the replacement of the invariant arginine on strand βB_2 by a tyrosine whose smaller side chain and different orientation enable deeper binding within the pocket. As a consequence of this deeper binding and of the different conformation of the αA_2 helix, the sulfate ion is more accessible on the side than on the top of the phosphoresidue-binding pocket, contrasting strongly with the $SH2_1$ domain. Strikingly, this side opening creates a direct path between the two phosphoresidue-binding pockets of the $SH2_1$ and $SH2_2$ domains (Fig. 3*C*).

Both $SH2_1$ and $SH2_2$ Participate in the interaction of Spt6 with RNAPII—To examine the role of both SH2 domains in the interaction of Spt6 with RNAPII, we performed GST pull-down experiments on yeast extract using GST-fused Spt6 constructs. Retention of RNAPII by the different constructs was monitored with antibodies directed against the polymerase CTD. Nonspecific binding was excluded because GST alone bound to glutathione-Sepharose was unable to retain

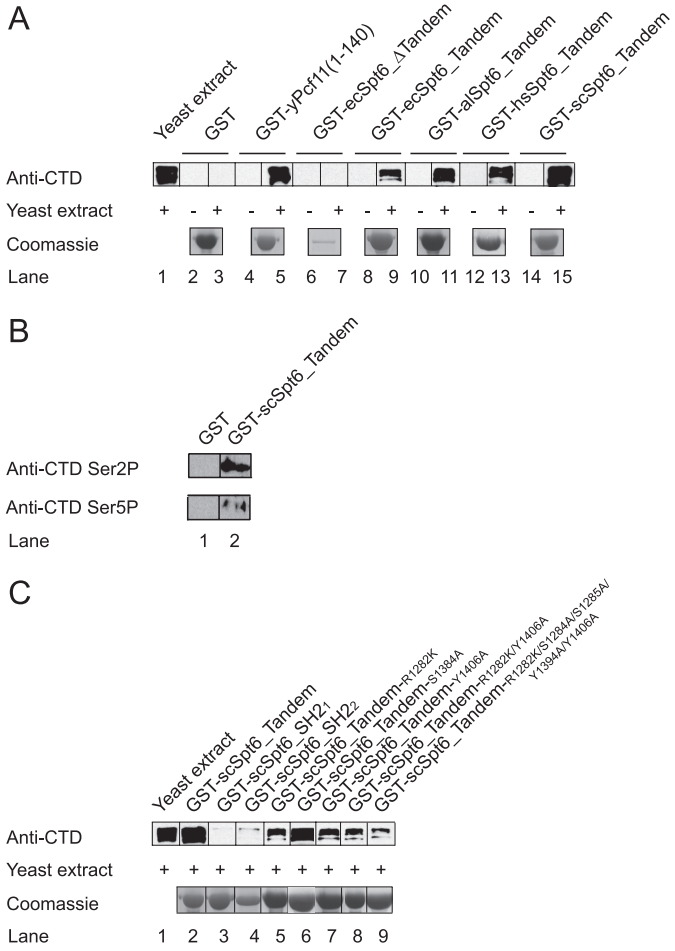

FIGURE 4. **GST pulldowns on yeast extract.** GST pulldowns were carried out using various GST-fused Spt6 constructs in the presence or absence of yeast extract. Binding of RNAPII was monitored by anti-CTD antibodies. The yeast extract control loaded (*lane 1*) corresponds to 0.1 μl of extract, whereas the quantity loaded after pulldown and washes corresponds to the equivalent of 2.5 μl of extract. Coomassie-stained samples of the different proteins used are shown. *A*, GST pulldowns made with GST alone (*lanes 2* and *3*) or fused to the CTD-interacting domain of the yeast termination factor Pcf11 (*lanes 4* and *5*) or to various constructs of Spt6 from *E. cuniculi* (*lanes 6–9*), *A. locustae* (*lanes 10* and *11*), *H. sapiens* (*lanes 12* and *13*), and *S. cerevisiae* (*lanes 14* and *15*). Both Pcf11 and the tandem SH2 are able to specifically retain the polymerase. *B*, analysis of phosphospecificity using anti-Ser^2(P) and anti-Ser^5(P) antibodies. A slight increase in binding to the Ser^2-phosphorylated form was observed. *C*, GST pulldowns performed on the yeast Spt6 (i) wild-type tandem SH2 (*lane 2*), (ii) SH2$_1$ domain (*lane 3*), (iii) SH2$_2$ domain (*lane 4*), and mutants of phosphate-binding residues from both domains in the context of the entire tandem SH2 (*lanes 5–9*). The results show that the entire tandem SH2 is required for RNAPII binding. Mutation of phosphate-binding determinants shows a decrease in binding, suggesting, that interaction with RNAPII is more extensive. For the *E. cuniculi* (*ec*) constructs, the N-terminal and the tandem SH2 domains span residues 1–725 and 724–894, respectively. The *A. locustae* (*al*) tandem SH2 construct spans residues 783–957. The human (*hs*) construct spans residues 1316–1727. For the *S. cerevisiae* (*sc*) constructs, the tandem SH2, SH2$_1$, and SH2$_2$ domains span residues 1231–1451, 1231–1350, and 1339–1451, respectively.

the RNAPII present in yeast extract (Fig. 4*A*, *lanes 2* and *3*). We then used the CTD-interacting domain of yeast Pcf11 as a positive control and showed that this protein is able to retain the RNAPII (Fig. 4*A*, *lanes 4* and *5*). We next investigated the capacity of Spt6 to retain RNAPII. A construct of *E. cuniculi* Spt6 lacking only the tandem SH2 showed no retention (Fig. 4*A*, *lanes 6* and *7*). In contrast, the tandem SH2 domains from *E. cuniculi*, *A. locustae*, *Homo sapiens*, and *Saccharomyces cerevisiae* were all able to retain the RNAPII (Fig. 4*A*, *lanes 8–15*). Antibodies specific for CTD phosphorylation on either Ser^2 or Ser^5 were used for analyzing phosphospecificity, showing an apparent increase in binding for the form phosphorylated on Ser^2 (Fig. 4*B*).

We next investigated the importance of both SH2 domains for binding to RNAPII. A GST pulldown assay using a yeast construct spanning only the SH2$_1$ domain was unable to retain significant amounts of RNAPII (Fig. 4*C*, *lane 3*). Similarly, yeast SH2$_2$ alone showed almost no ability to retain RNAPII (Fig. 4*C*, *lane 4*). We next asked whether the two phosphate-binding pockets of the tandem SH2 domains are important for recognition. We first changed the invariant arginine scArg^{1282} in βB$_1$ of the yeast SH2$_1$ domain to lysine. This mutant, although it only partially removes the phosphate-binding determinants of SH2$_1$, was impaired about 5-fold in retaining RNAPII (Fig. 4*C*, *lane 5*). In contrast, in the case of the yeast SH2$_2$, a change of the invariant arginine of the βB$_2$ strand to alanine (scSer^{1384}, equivalent to alTyr^{906}), had no effect on RNAPII binding, in agreement with our structural results showing that this residue is most likely not involved in phosphate recognition (Fig. 4*C*, *lane 6*).

We therefore altered another putative phospho-binding residue, scTyr^{1406}, from the βD$_2$ strand of the SH2$_2$ domain to alanine. In this case, the mutant showed the same loss of interaction with RNAPII of that observed with the scR1282K mutant (Fig. 4*C*, *lane 7*). Interestingly, a double mutant scR1282K/Y1406A showed no additive effect on RNAPII binding (Fig. 4*C*, *lane 8*), suggesting that either the remaining phospho-binding residues are sufficient to enable weak binding or that contacts occurring outside the phospho-binding pockets may stabilize this weak interaction. To verify this hypothesis, we constructed an additional mutant that removes all putative phospho-binding side chains in the tandem SH2 domains (scR1282K/S1284A/S1285A/Y1394A/Y1406A). This mutant also showed a reduced level of RNAPII binding (Fig. 4*C*, *lanes 9*). Taken together, these results suggest that the interaction between Spt6 tandem SH2 domains and RNAPII is more extensive than just phosphoresidue recognition.

Tandem SH2 Domains and SH2$_2$ Domain Alone Are Critical for Spt6 Function In Vivo—Our structural and biochemical results show the importance of the tandem SH2 domains for interaction with RNAPII. The SH2$_2$ domain appears as essential as the SH2$_1$ for this activity. To investigate the requirement for these domains *in vivo*, we have created two yeast mutants lacking either both of the tandem SH2 domains or only the SH2$_2$ domain and analyzed them for mutant phenotypes. Our results show that both deletion mutants are viable, although they grow much more slowly than wild type and have several mutant phenotypes, including impaired growth at high (37 °C) and low (16 °C) temperatures, suppression of the insertion mutation *his4–912*δ (Spt phenotype (9)), cryptic initiation at a *FLO8-HIS3* reporter (48), and sensitivity to hydroxyurea, phleomycin, and caffeine (Fig. 5*A*). Our results with the mutant lacking both SH2 domains agree in general with previous studies of this deletion (37). Our finding that a mutant lacking only the SH2$_2$ domain has severe mutant phe-

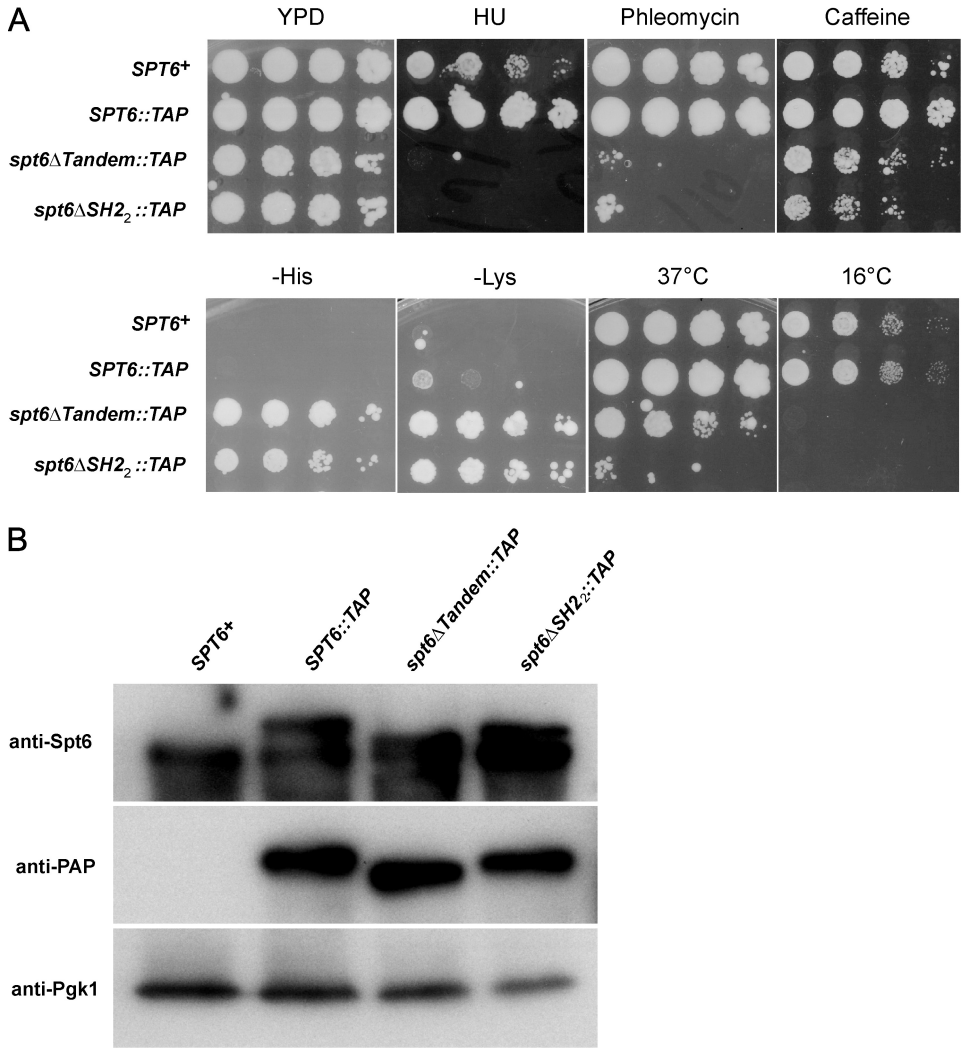

FIGURE 5. ***In vivo* requirement of the tandem SH2 in yeast Spt6.** *A*, strains were grown to saturation in YPD, serially diluted 10-fold, spotted on the indicated media, and incubated for 6 days. The strains used were FY2809, FY28010, FY2811, and FY2812 (supplemental Table 2). Growth on -His indicates cryptic transcription initiation of the *FLO8-HIS3* reporter (48), and growth on -Lys indicates suppression of the *lys2–128δ* insertion mutation (Spt$^-$ phenotype) (9). *B*, Western blot analysis of Spt6 levels. Protein extracts were prepared from strains FY653, FY2796, FY2797, and FY2798 (supplemental Table 2) as described previously (48). The *top panel* shows a blot probed with α-Spt6 antibody (courtesy of Laura McCollough and Tim Formosa). In this *panel*, in *lanes 2*, *3*, and *4*, two bands are visible because the strains are diploid. The *upper band* is the TAP-tagged Spt6, and the *lower band* is untagged Spt6. The middle *panel is* probed with α-PAP antibody (Sigma P1291), and the *bottom panel s*hows the Pgk1 loading control.

notypes indicates that this noncanonical SH2 domain plays a critical role in Spt6 function.

To determine whether any of the mutant phenotypes might be due to altered levels of Spt6 protein, we performed Western analysis on the diploid strains containing each TAP-tagged allele. Our results (Fig. 5*B*) show that the deletions do not have a significant effect on Spt6 protein levels. Thus, loss of either both SH2 domains or just the $SH2_2$ domain severely impairs Spt6 function, demonstrating the importance of these domains *in vivo*.

Two Consecutive Phosphorylated CTD Repeats Are Not Sufficient for Binding to the Tandem SH2—The C-terminal region of mammalian Spt6 has been shown to bind directly to the RNAPII CTD upon hyperphosphorylation of the CTD repeats on Ser2 (17, 23). We reasoned that the recognition of a Ser^2 hyperphosphorylation state most likely implies that the tandem SH2 domains bind consecutive phosphorylated repeats because recognition of remote phosphorylated CTD repeats could select for low Ser^2 phosphorylation. Modeling shows that two phosphorylated repeats could indeed bind to the tandem SH2 domains (supplemental Fig. 4). In this model, binding would require an extended conformation of the peptide linking both phosphoserines and would also be dependent on the noncanonical features of the $SH2_2$, notably the opening between the two phospho-binding pockets and the deeper positioning of the phosphate within the $SH2_2$ binding pocket, as observed for the sulfate ion in our structure.

We have experimentally investigated this binding mode of two consecutive phosphorylated CTD repeats to the tandem SH2 domains by using microcalorimetry (ITC) and Thermofluor technologies. Peptides bearing no phosphoserines or two consecutive phosphorylations on Ser^2, Ser^5, or Ser^7 were used, with a few flanking residues on both sides of the phosphoresidues to enable interaction with the putative second binding pockets of the SH2 domains as in a two-pronged mechanism. Despite the fact that both techniques used rely

on different technologies, none of the peptides was shown to bind to the tandem SH2 domains. These results, which show that two CTD repeats cannot recapitulate RNAPII binding, are in agreement with our mutational data which indicate that the recognition of the phosphorylated RNAPII by the Spt6 C-terminal region requires extensive interaction of these macromolecules.

DISCUSSION

SH2 domains are found almost exclusively in metazoans where they serve as phosphotyrosine-binding motifs and regulate the activity of protein tyrosine kinases that participate in signaling pathways (52, 53). The discovery that Spt6 contains the only SH2 domain found in yeast (36) and the fact that Spt6 most likely evolved from the bacterial transcription factor Tex (25, 54), suggested that this SH2 domain represents an ancestor of the SH2 domains of multicellular organisms. This view of an ancestral SH2 motif has been reinforced by the finding that the mammalian Spt6 SH2 domain interacts directly with RNAPII upon phosphorylation of serine rather than tyrosine residues in its CTD repeats (17, 23).

We show here that this view is oversimplified and that the Spt6 C-terminal region is actually composed of two SH2 domains arranged in tandem. Superposition of these domains suggests that the tandem arrangement arose by duplication (supplemental Fig. 5). Yet, both domains are highly divergent in the details of their organization. Whereas the $SH2_1$ domain has characteristics that are often found in SH2 domains from multicellular organisms, the $SH2_2$ domain harbors features that appear unique in the family of SH2 domains. The conservation of this tandem SH2 throughout evolution, from yeast to man, highlights its functional importance. Our *in vivo* data, which show that the tandem SH2 domains are required for Spt6 function, clearly confirm this view.

The *in vivo* importance of the tandem SH2 domains is in agreement with the functional role of Spt6 during elongation. In particular, the distribution of the Spt6 and Iws1 proteins on the promoters and bodies of genes (24) suggests that these proteins travel together with RNAPII. Previous results on mammalian Spt6 (17, 23) and our current results on yeast Spt6 show that the conserved C-terminal tandem SH2 domain of Spt6 has the ability to bind RNAPII. The known interaction of Iws1 with Spt6 (17–22) provides a means for Iws1 to travel with RNAPII. Importantly, mutation of the mammalian $SH2_1$ domain causes the same defects as those observed upon mammalian Iws1 depletion (17). Therefore the interaction of the Spt6 tandem SH2 domains with RNAPII is not only critical for Spt6 but most likely also for Iws1 function.

Importantly, our biochemical analyses show that the tandem, but not the individual SH2 domains, interact with RNAPII. As such, the tandem should be seen as a single functional unit. In agreement, it has been shown that binding of doubly phosphorylated peptides to tandem SH2 domains, as in the case of the SH-PTP2 phosphatase and the ZAP-70 protein tyrosine kinase, causes a significant increase in binding affinity (34, 35). Our structural data reveals that both Spt6 SH2 domains have retained determinants for phosphate binding. Mutation of the $scSer^{1384}$ residue (equivalent of $alTyr^{906}$), which is located within the phospho-binding pockets but that is not predicted to bind phosphates, does not affect binding. In contrast, mutation of putative phosphate-binding residues decreases RNAPII binding. Yet, these mutations do not abolish binding as observed with the individual SH2 domains. This suggests that additional interactions are responsible for the observed weaker binding. It cannot be excluded that interactions within the phospho-binding pockets between the Spt6 main chain atoms and the phosphates, such as those observed in our structure, could contribute to this weaker interaction. However, it appears likely that interactions occurring outside the pockets also contribute to interaction and to the weaker binding observed.

The absence of interaction between short phosphorylated tandem CTD repeats and the Spt6 tandem SH2 domains also supports this view. Specifically, these latter experiments were performed with peptides long enough to enable their binding to the second binding pocket of the SH2 domains, assuming a canonical way of binding. Actually, there is very little evidence that the specific recognition of phosphoproteins by SH2 domains is only based on the binding of a phosphoresidue and its flanking residues. So far, the vast majority of binding studies have been carried out on small phosphopeptides rather than full phosphoproteins. However, this view has recently changed with the determination of the structure of the FGFR1/phospholipase Cγ complex, where a second interaction between a SH2 domain and its target phosphoprotein has been observed and shown to be essential for high affinity binding (33). Our results, together with previous observations made with the mouse Spt6 protein (23), argue in favor of such a hypothesis.

Altogether, the results presented here reveal that the recognition of the phosphorylated CTD of the elongating RNAPII by the C-terminal region of Spt6 does not make use of a simple mechanism based on a single SH2 domain. Rather, this recognition requires a highly intricate mechanism involving a noncanonical tandem SH2 domain. The conservation of this tandem SH2 domain throughout eukaryotic evolution and our *in vivo* analyses demonstrate that this domain is essential for the function of the histone chaperone and elongation factor Spt6 which performs its role in the wake of the RNAPII.

Acknowledgments—We thank members of the ESRF-EMBL joint structural biology groups for the use of the ESRF beamline facilities and help during data collection. We also thank Eric Ennifar for help during ITC measurements, Marc Vigneron for the kind gift of the CTD peptides, Laura McCollough and Tim Formosa for Spt6 antisera, Céline Faux and Bertrand Séraphin for help during the preparation of the yeast extract, and Irwin Davidson for fruitful discussions and critical reading of the manuscript.

REFERENCES

1. Li, B., Carey, M., and Workman, J. L. (2007) *Cell* **128,** 707–719
2. Perales, R., and Bentley, D. (2009) *Mol. Cell* **36,** 178–191
3. Saunders, A., Core, L. J., and Lis, J. T. (2006) *Nat. Rev. Mol. Cell Biol.* **7,** 557–567
4. Chapman, R. D., Heidemann, M., Hintermair, C., and Eick, D. (2008) *Trends Genet.* **24,** 289–296

5. Buratowski, S. (2009) *Mol. Cell* **36,** 541–546
6. Egloff, S., and Murphy, S. (2008) *Trends Genet.* **24,** 280–288
7. Phatnani, H. P., and Greenleaf, A. L. (2006) *Genes Dev.* **20,** 2922–2936
8. Meinhart, A., Kamenski, T., Hoeppner, S., Baumli, S., and Cramer, P. (2005) *Genes Dev.* **19,** 1401–1415
9. Winston, F., Chaleff, D. T., Valent, B., and Fink, G. R. (1984) *Genetics* **107,** 179–197
10. Clark-Adams, C. D., and Winston, F. (1987) *Mol. Cell. Biol.* **7,** 679–686
11. Neigeborn, L., Celenza, J. L., and Carlson, M. (1987) *Mol. Cell. Biol.* **7,** 672–678
12. Bortvin, A., and Winston, F. (1996) *Science* **272,** 1473–1476
13. Adkins, M. W., and Tyler, J. K. (2006) *Mol. Cell* **21,** 405–416
14. Kaplan, C. D., Laprade, L., and Winston, F. (2003) *Science* **301,** 1096–1099
15. Ardehali, M. B., Yao, J., Adelman, K., Fuda, N. J., Petesch, S. J., Webb, W. W., and Lis, J. T. (2009) *EMBO J.* **28,** 1067–1077
16. Endoh, M., Zhu, W., Hasegawa, J., Watanabe, H., Kim, D. K., Aida, M., Inukai, N., Narita, T., Yamada, T., Furuya, A., Sato, H., Yamaguchi, Y., Mandal, S. S., Reinberg, D., Wada, T., and Handa, H. (2004) *Mol. Cell. Biol.* **24,** 3324–3336
17. Yoh, S. M., Cho, H., Pickle, L., Evans, R. M., and Jones, K. A. (2007) *Genes Dev.* **21,** 160–174
18. Fischbeck, J. A., Kraemer, S. M., and Stargell, L. A. (2002) *Genetics* **162,** 1605–1616
19. Liu, Z., Zhou, Z., Chen, G., and Bao, S. (2007) *Biochem. Biophys. Res. Commun.* **353,** 47–53
20. Gavin, A. C., Bösche, M., Krause, R., Grandi, P., Marzioch, M., Bauer, A., Schultz, J., Rick, J. M., Michon, A. M., Cruciat, C. M., Remor, M., Höfert, C., Schelder, M., Brajenovic, M., Ruffner, H., Merino, A., Klein, K., Hudak, M., Dickson, D., Rudi, T., Gnau, V., Bauch, A., Bastuck, S., Huhse, B., Leutwein, C., Heurtier, M. A., Copley, R. R., Edelmann, A., Querfurth, E., Rybin, V., Drewes, G., Raida, M., Bouwmeester, T., Bork, P., Seraphin, B., Kuster, B., Neubauer, G., and Superti-Furga, G. (2002) *Nature* **415,** 141–147
21. Krogan, N. J., Kim, M., Ahn, S. H., Zhong, G., Kobor, M. S., Cagney, G., Emili, A., Shilatifard, A., Buratowski, S., and Greenblatt, J. F. (2002) *Mol. Cell. Biol.* **22,** 6979–6992
22. Lindstrom, D. L., Squazzo, S. L., Muster, N., Burckin, T. A., Wachter, K. C., Emigh, C. A., McCleery, J. A., Yates, J. R., 3rd, and Hartzog, G. A. (2003) *Mol. Cell. Biol.* **23,** 1368–1378
23. Yoh, S. M., Lucas, J. S., and Jones, K. A. (2008) *Genes Dev.* **22,** 3422–3434
24. Kim, M., Ahn, S. H., Krogan, N. J., Greenblatt, J. F., and Buratowski, S. (2004) *EMBO J.* **23,** 354–364
25. Kaplan, C. D., Morris, J. R., Wu, C., and Winston, F. (2000) *Genes Dev.* **14,** 2623–2634
26. Andrulis, E. D., Guzmán, E., Döring, P., Werner, J., and Lis, J. T. (2000) *Genes Dev.* **14,** 2635–2649
27. Adelman, K., Wei, W., Ardehali, M. B., Werner, J., Zhu, B., Reinberg, D., and Lis, J. T. (2006) *Mol. Cell. Biol.* **26,** 250–260
28. Saunders, A., Werner, J., Andrulis, E. D., Nakayama, T., Hirose, S., Reinberg, D., and Lis, J. T. (2003) *Science* **301,** 1094–1096
29. Pawson, T., and Nash, P. (2003) *Science* **300,** 445–452
30. Kuriyan, J., and Cowburn, D. (1997) *Annu. Rev. Biophys. Biomol. Struct.* **26,** 259–288
31. Songyang, Z., Shoelson, S. E., Chaudhuri, M., Gish, G., Pawson, T., Haser, W. G., King, F., Roberts, T., Ratnofsky, S., Lechleider, R. J., *et al.* (1993) *Cell* **72,** 767–778
32. Waksman, G., Shoelson, S. E., Pant, N., Cowburn, D., and Kuriyan, J. (1993) *Cell* **72,** 779–790
33. Bae, J. H., Lew, E. D., Yuzawa, S., Tomé, F., Lax, I., and Schlessinger, J. (2009) *Cell* **138,** 514–524
34. Eck, M. J., Pluskey, S., Trüb, T., Harrison, S. C., and Shoelson, S. E. (1996) *Nature* **379,** 277–280
35. Hatada, M. H., Lu, X., Laird, E. R., Green, J., Morgenstern, J. P., Lou, M., Marr, C. S., Phillips, T. B., Ram, M. K., Theriault, K., *et al.* (1995) *Nature* **377,** 32–38
36. Maclennan, A. J., and Shaw, G. (1993) *Trends Biochem. Sci.* **18,** 464–465
37. Dengl, S., Mayer, A., Sun, M., and Cramer, P. (2009) *J. Mol. Biol.* **389,** 211–225
38. Romier, C., Ben Jelloul, M., Albeck, S., Buchwald, G., Busso, D., Celie, P. H., Christodoulou, E., De Marco, V., van Gerwen, S., Knipscheer, P., Lebbink, J. H., Notenboom, V., Poterszman, A., Rochel, N., Cohen, S. X., Unger, T., Sussman, J. L., Moras, D., Sixma, T. K., and Perrakis, A. (2006) *Acta Crystallogr. D Biol. Crystallogr.* **62,** 1232–1242
39. Otwinowski, Z., and Minor, W. (1997) *Methods in Enzymology* (Carter, Jr., C. W., and Sweet, R. M. eds) pp. 307–326, Academic Press, New York
40. Vonrhein, C., Blanc, E., Roversi, P., and Bricogne, G. (2007) *Methods Mol. Biol.* **364,** 215–230
41. Abrahams, J. P., and Leslie, A. G. (1996) *Acta Crystallogr. D Biol. Crystallogr.* **52,** 30–42
42. Emsley, P., and Cowtan, K. (2004) *Acta Crystallogr. D Biol. Crystallogr.* **60,** 2126–2132
43. CCP4 (1994) *Acta Crystallogr. D Biol. Crystallogr.* **50,** 760–763
44. Seraphin, B., and Rosbash, M. (1989) *Cell* **59,** 349–358
45. Besse, S., Vigneron, M., Pichard, E., and Puvion-Dutilleul, F. (1995) *Gene Expr.* **4,** 143–161
46. Van Driessche, B., Tafforeau, L., Hentges, P., Carr, A. M., and Vandenhaute, J. (2005) *Yeast* **22,** 1061–1068
47. Rose, M. D., Winston, F., and Hieter, P. (1990) *Laboratory Course Manual for Methods in Yeast Genetics*, Cold Spring Harbor Laboratory, Cold Spring Harbor, NY
48. Cheung, V., Chua, G., Batada, N. N., Landry, C. R., Michnick, S. W., Hughes, T. R., and Winston, F. (2008) *PLoS Biol.* **6,** e277
49. Katinka, M. D., Duprat, S., Cornillot, E., Méténier, G., Thomarat, F., Prensier, G., Barbe, V., Peyretaillade, E., Brottier, P., Wincker, P., Delbac, F., El Alaoui, H., Peyret, P., Saurin, W., Gouy, M., Weissenbach, J., and Vivarès, C. P. (2001) *Nature* **414,** 450–453
50. Romier, C., James, N., Birck, C., Cavarelli, J., Vivarès, C., Collart, M. A., and Moras, D. (2007) *J. Mol. Biol.* **368,** 1292–1306
51. Holm, L., Kääriäinen, S., Rosenström, P., and Schenkel, A. (2008) *Bioinformatics* **24,** 2780–2781
52. Filippakopoulos, P., Müller, S., and Knapp, S. (2009) *Curr. Opin Struct. Biol.* **19,** 643–649
53. Liu, B. A., Jablonowski, K., Raina, M., Arcé, M., Pawson, T., and Nash, P. D. (2006) *Mol. Cell* **22,** 851–868
54. Johnson, S. J., Close, D., Robinson, H., Vallet-Gely, I., Dove, S. L., and Hill, C. P. (2008) *J. Mol. Biol.* **377,** 1460–1473
55. Bond, C. S., and Schüttelkopf, A. W. (2009) *Acta Crystallogr. D Biol. Crystallogr.* **65,** 510–512